

# DYNAMIC BEHAVIOR OF METAL-PLATE-CONNECTED WOOD TRUSS JOINTS

By Scott M. Kent,<sup>1</sup> Rakesh Gupta,<sup>2</sup> Member, ASCE,  
and Thomas H. Miller,<sup>3</sup> Member, ASCE

**ABSTRACT:** The objective of the paper is to describe the behavior of metal-plate-connected (MPC) tensile and heel joints under seismic and cyclic loads. A proposed sequential phase displacement (SPD) loading standard was also used to determine dynamic characteristics (energy dissipation, damping ratio, and cyclic stiffness) of MPC joints. Strengths and stiffnesses of MPC joints after the seismic and SPD loadings were compared to those properties for a control group of joints tested to failure under a static ramp load. Strength degradation was not observed in tensile and heel joints as a result of the seismic loads. Stiffness degradation was observed in the heel joint as a result of the large artificial earthquake loads and in both tensile and heel joints as a result of the SPD loading. Dynamic properties from the SPD loading depended on the magnitude of displacement. The damping ratio and energy dissipation increased as the SPD loading progressed, whereas the cyclic stiffness decreased. Cyclic loading also showed a significant effect on the strength of MPC joints depending on the amplitude of the cycles.

## INTRODUCTION

Metal-plate-connected (MPC) wood trusses, although exposed to dynamic loadings from wind and earthquakes, are designed predominately based on their response to static loads. The prevalence of MPC trusses in construction and numerous full-scale truss tests conducted by truss manufacturers and others have not resulted in a widespread understanding of their behavior in service, especially under seismic and high wind forces. Most of the research on the structural behavior of MPC joints has focused on their static behavior. Significant advances have been made in the area of modeling the earthquake behavior of timber shear walls and roof diaphragms in recent years, but research on the response of MPC joints to seismic forces has largely been ignored. Connections are primary factors controlling the response of structural assemblies; therefore, results from connection tests will continue to be significant in understanding the behavior of buildings during dynamic loading events.

The Truss Plate Institute (TPI) provides a widely recognized standard ("National" 1995) for the evaluation of the behavior of MPC joints under static axial loads only. ASTM also provides a standard for determining tensile strength and stiffness characteristics of MPC tensile joints under static loads (*Standard* 1996b). These evaluations are inadequate because actual joints (having different configurations) experience different loading (cyclic, combined, reversed) conditions in service. Dolan (1994) proposed a pseudodynamic sequential phased displacement (SPD) loading for wood connections based on a quasi-static test procedure developed for masonry shear walls (Porter 1987). The purpose of the SPD loading is to provide a consistent method for the determination of dynamic properties such as equivalent viscous damping ratio, ductility, and cyclic stiffness.

<sup>1</sup>Res. Coordinator, Wood Sci. and Tech. Inst. (N.S.), Ltd., 850 SW 15th Ave., Ste. 1B, Corvallis, OR 97333; formerly, Grad. Res. Asst., Depts. of Forest Products and Civ., Constr., and Envir. Engrg., Oregon State Univ., Corvallis, OR 97331.

<sup>2</sup>Asst. Prof., Dept. of Forest Products, Oregon State Univ., Corvallis, OR.

<sup>3</sup>Assoc. Prof., Dept. of Civ., Constr., and Envir. Engrg., Oregon State Univ., Corvallis, OR.

Note. Associate Editor: Dan L. Wheat. Discussion open until January 1, 1998. To extend the closing date one month, a written request must be filed with the ASCE Manager of Journals. The manuscript for this paper was submitted for review and possible publication on September 12, 1996. This paper is part of the *Journal of Structural Engineering*, Vol. 123, No. 8, August, 1997. ©ASCE, ISSN 0733-9445/97/0008-1037-1045/\$4.00 + \$.50 per page. Paper No. 14073.

Numerous studies (Gupta et al. 1996) have been conducted on static testing of MPC joints, but only a few efforts on the dynamic testing of MPC joints were found (Sletteland et al. 1977; Tokuda et al. 1979; Hayashi et al. 1980; Dagher et al. 1991; Buchanan and Dean 1994; Emerson and Fridley 1996). In each of these studies, the tensile joint alone was tested under repeated axial loads. In MPC wood trusses, other joints are also critical in the overall behavior of the truss. Evaluations from these previous efforts are inadequate to determine the behavior of MPC joints during earthquake loadings.

Most light-frame wood structures have a fundamental natural frequency of vibration between 1.2 and 18 Hz (Foliente and Zacher 1994), which coincides with the dominant frequencies of many seismic events. To limit dynamic amplifications, it is important that the structure respond as a highly damped system. To add to the somewhat limited energy dissipation provided by the structural members alone, connections can be effectively designed to increase the energy dissipation of the entire structure. Understanding the hysteresis behavior of wood joints is necessary to model the dynamic response of complex timber structural systems.

The objective of this study is to characterize the structural behavior and failure modes of MPC tension-splice and heel wood truss joints under various dynamic loading conditions. This is a necessary first step toward predicting truss joint behavior and subsequently predicting the behavior of a truss and a system of trusses under dynamic loads.

## MATERIALS AND METHODS

Two types of joints were tested in this study: tension-splice joints (TSJ) and heel joints (HJ). Table 1 lists the groups of tests examined and provides sample sizes for each group. Two different batches of the same type of plate were used for TSJ tests because the supply of 76 × 102 mm metal plates initially available, henceforth referred to as batch 1, was exhausted. New plates, batch 2, having exactly the same tooth configuration as batch 1, were ordered from the same supplier. The TSJs were connected using 76 × 102 mm plates, whereas the heel joints were connected using 76 × 127 mm plates. Table 2 lists characteristics of the metal plate connectors. Overall length of a TSJ was approximately 1 m, and the heel joint's top and bottom chord were both about 0.5 m long.

All test joints were fabricated from machine-stress-rated Douglas fir (1800f-1.6E) lumber that was conditioned at 21°C and 65% relative humidity to an equilibrium moisture content of approximately 14%. One plate was pressed at a time using a hydraulic press. Plates were pressed until no gap was visible

**TABLE 1. Sample Size and Test Types for MPC Joints**

Test (1)	Batch* (2)	Sample size (3)
(a) Tension-splice joint		
Control group (static test)	1	9
Control group (static test)	2	9
Northridge earthquake loads	1	10
Large earthquake loads	2	9
SPD loads	1	8
Cyclic loads	2	20
(b) Heel joints		
Control group (static test)	2	9
Large earthquake loads	2	10
SPD loads	2	9
Cyclic loads	2	25

\*Two different batches of the same type of plate.

**TABLE 2. Physical Properties of Metal-Plate Connectors\***

Parameter (1)	Batch 1 (2)	Batch 2 (3)
Yield strength (MPa)	241–379 <sup>b</sup>	355
Ultimate strength (MPa)	365–427 <sup>b</sup>	416
Percent elongation at failure (%)	25–39 <sup>b</sup>	31.5
Thickness (mm)	0.9	0.9
Thickness (gauge)	20	20
Tooth length (mm)	6	6
Tooth width (mm)	3	3
Slot length (mm)	6	6
Slot width (mm)	3	3

\*All plates supplied by Alpine Engineered Products, Inc., Pompano Beach, Fla.

<sup>b</sup>Material properties were not determined; therefore, a sample of values for the properties expected for ASTM A446-89 Grade B steel is shown.

between the plate and wood. After fabrication, the joints were stored in the environment room again for a minimum of seven days before testing ("National" 1995). Specific gravity and moisture content were measured according to ASTM Standards D2395-93 (Standard 1996c) and D4442-92 (Standard 1996a), respectively. The modulus of elasticity of the wood for the MPC joints was measured using an E-computer (Model 390, Metriguard, Pullman, Wash.).

**Apparatus**

A horizontal testing frame, developed by Gupta and Gebremedhin (1990), which allows for testing a range of joint configurations, and a 49-kN capacity materials testing system (MTS) dynamic hydraulic actuator were used to apply the loads to the joints. Fig. 1 shows a TSJ positioned in the testing frame. Relative displacements between the two wood members were measured by two alternating current, linear variable differential transducers (LVDTs) placed on either side of the TSJ.

Fig. 2 shows an HJ positioned in the testing apparatus. The joints were tested under axial loads only, but small, unintentional eccentricities in the loads introduced moments in the HJs. Moments induced by bending of the top chord under gravity loads were not simulated. The two LVDTs shown in Fig. 2 were used to measure the longitudinal deflection of the top chord relative to the bottom chord and the rotation of the top chord in relation to the bottom chord of the HJ. The support for the HJ was designed to simulate a roller support. The width of the support was 140 mm to simulate a typical bearing wall in a residential structure. The support was also able to restrain uplift caused by tensile loadings in the top chord during the sequential phased displacement (SPD) loading. As shown in Fig. 2, braces were used to restrain movement of the

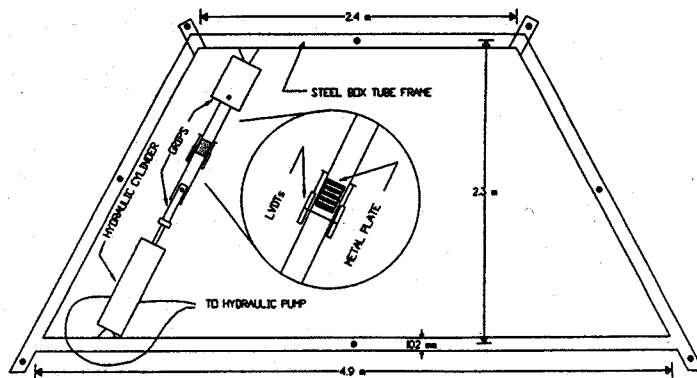


**FIG. 1. Test Setup for Tension Splice Joint**

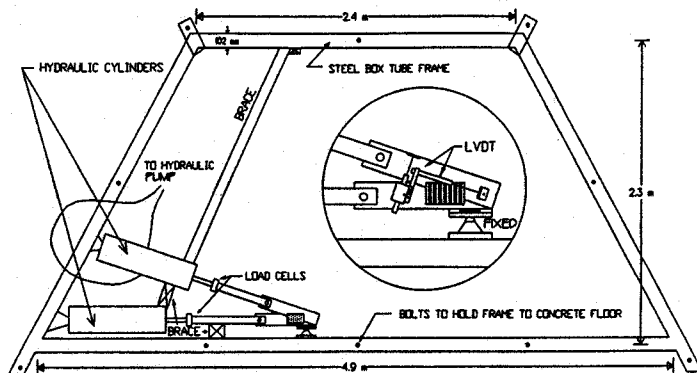


**FIG. 2. Test Setup for Heel Joint**

MTS cylinder as compressive loads were applied to the top chord through a 19-mm-diameter pin.

The MTS system used in this study was capable of making feedback corrections (to both load and deflection) at a rate of 500 Hz.

**Loading Conditions**

Loading conditions for TSJ and HJ tests listed in Table 1 are described as follows. For all loading cases 10 joints were actually tested but in some cases data for one or two joints were lost due to technical problems.

**Static Tests**

A linearly increasing tensile ramp load of 3.5 kN/min was applied axially to tensile joints to cause failure in 8–10 min. A linearly increasing compressive ramp load of 5.3 kN/min was applied to the top chord of heel joints to cause failure in 5–6 min.

**Northridge Earthquake Loads**

TSJs were subjected to a force time history to simulate the effects of the Northridge earthquake that occurred near Santa Monica, Calif. (Richter magnitude of 6.4, STA No. 24538). A 9.1-m-span Fink truss composed of 38 × 89-mm Douglas fir (modulus of elasticity of 11 GPa) was modeled using a linear finite-element program (SAP90 1995) to estimate forces in the TSJ (Kent 1996). The 90° (azimuth) horizontal component and the vertical component of the Northridge earthquake, which had maximum accelerations of 0.90 and 0.23 g, respectively, were analyzed separately and superimposed to obtain the time-history response of the force at the tensile joint. The calculated target response of the TSJ is shown in Fig. 3 along with the peak portions of the target and actual force-time histories in the joint to demonstrate how well the loading system was able to mimic the target response. A ramp load of 3.5 kN/min was

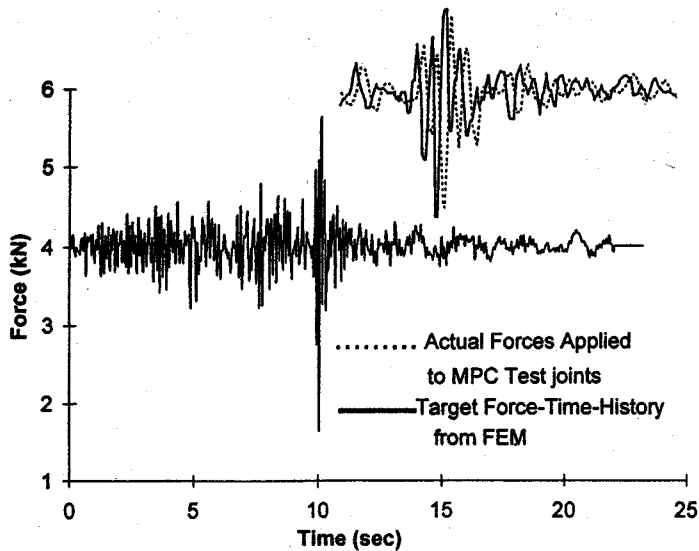


FIG. 3. Target Force-Time History for Tension-Splice Joint During Northridge Earthquake

first applied to the joints until the estimated dead load force of 4 kN was reached. The earthquake forces were then applied for a duration of 30 s, followed by a continuation of the ramp load until the joints failed. The earthquake force time history alone was not sufficient to cause the joints to fail. HJs were not tested under this loading condition because even forces from a large artificial earthquake (explained in the next section) did not cause any damage in the HJ.

#### Large Artificial Earthquake Loads

A large artificial earthquake time history was generated using WES-RASCAL (Silva and Lee 1987) and the Uniform Building Code (UBC) design spectrum ("Structural" 1994). The maximum horizontal and vertical accelerations were 1.0 and 0.67 *g*, respectively. This was then used in SAP90 to determine the time-history response for TSJ and HJ. Calculated target force-time responses of TSJ and HJ are shown in Figs. 4 and 5, respectively. The artificial earthquake forces were then applied to TSJs and HJs in the laboratory. Again, a ramp load was applied until the estimated dead load force was reached. The earthquake forces were then applied followed by a ramp load until the joints failed.

#### Sequential Phased Displacement Loading

The sequential phased displacement (SPD) method (Dolan 1994; Porter 1987) was used to determine the dynamic properties (such as energy dissipation, damping ratio, and cyclic stiffness) of the MPC TSJs and HJs. The loading function

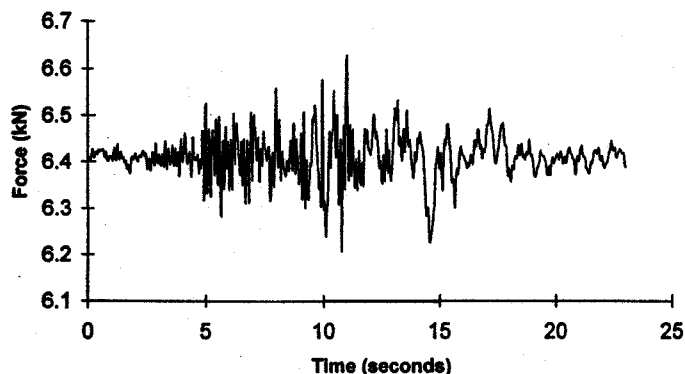


FIG. 4. Target Force-Time History for Tension-Splice Joint during Artificial Earthquake

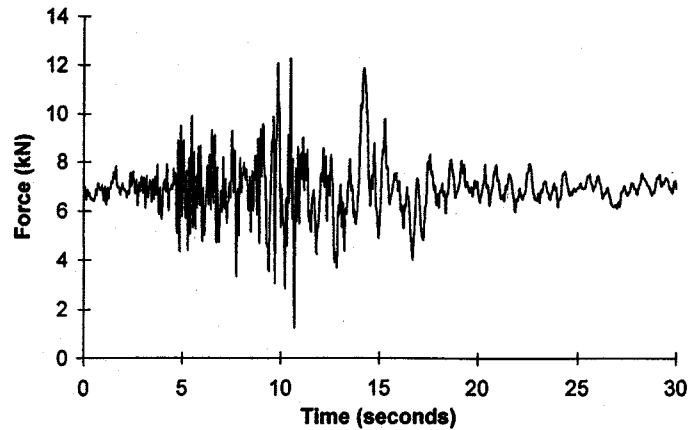


FIG. 5. Target Force-Time History for Top Chord of Heel Joint during Artificial Earthquake

combined fully reversed stabilizing cyclic displacements preceding degradation cycles at a frequency of 1 Hz, which approximates the expected overall response of a low-rise timber structure under a seismic or high wind event. The stabilizing and degradation cycles gradually increased, following the pattern shown in Fig. 6, which graphically displays a typical SPD loading function.

The SPD cycles are defined in terms of the yield displacement for the type of connection being studied. A yield displacement (displacement at one-third of the strength) of 0.15 mm from the static loading control group (batch 1), was used to scale the SPD cycles for TSJ. Originally the objective was to cause the joints to fail during the SPD tests, but the compressive load limit for the hydraulic actuator of approximately 45 kN was reached before failure occurred in the joints. Therefore, the joints were subjected to a maximum of 120 SPD cycles. Joints were then caused to fail under a ramp load of 3.5 kN/min to determine how the SPD loading affected the strength and stiffness of the MPC TSJs. Since the TSJ did not fail during the SPD loading due to wood-to-wood bearing, a full reversing load control test might be better suited for the joints and provide a more realistic loading.

A yield displacement (for axial deflection) of 0.18 mm from the control group, was used to scale the SPD cycles for HJ. After application of 120 SPD cycles, HJs were caused to fail under a ramp load of 5.3 kN/min to determine how the SPD loading affected the strength and stiffness.

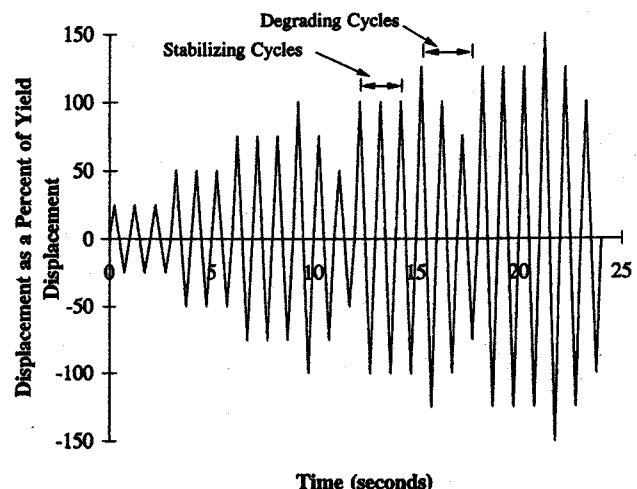


FIG. 6. Sequential Phased Displacement Loading Function (Dolan 1994; Porter 1987)

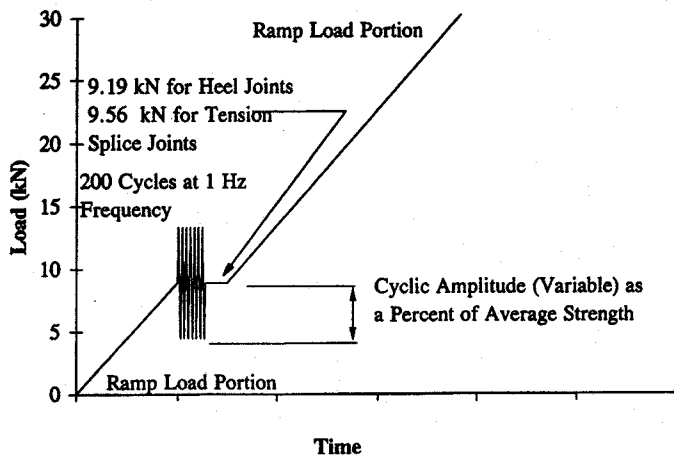


FIG. 7. Cyclic Loading Function for Tension-Splice and Heel Joints

### Cyclic Loads

To determine the effects of cyclic loading, a sinusoidal waveform with the baseline of the oscillations (centerline of the cycles) at one-third of the mean strength was applied for 200 cycles at a frequency of 1 Hz (Fig. 7). Three joints were typically tested at each amplitude level. The TSJs were tested with amplitudes of approximately 8, 12, 16, 18, 19, and 20% of the mean static strength (one extra joint was tested at 16% and one more at 25%). The HJs were tested with amplitudes of 5, 10, 15, 20, 25, 30, 33, 35, and 40% of the mean static strength. If the joint was still able to carry load after the cycles, the static ramp load was continued until failure.

## RESULTS AND DISCUSSION

### Statistical Methods

The mean strengths and stiffnesses of the TSJ and HJ for each dynamic loading are compared to those from a control group (static ramp load). A t-test procedure for comparing two sample means, assuming equal population variance, is used to analyze the strength and stiffness results. A two-sided p-value of 0.05 is chosen as the cutoff significance level.

### Tension Splice Joints

Strength, stiffness, specific gravity, and moisture content results for all TSJ tests are shown in Table 3, along with deflection at maximum load, yield displacement, modulus of elasticity, and failure modes. Mean strength for the cyclic loading tests is not given in this table because of the strength dependence on the amplitude of the cycles.

The dominant failure mode for the TSJs was tooth with-

drawal, although there were three instances where the metal plate connector failed in tension. The tooth withdrawal failure mode occurred as a result of the wood being crushed by the side of the teeth near the surface of the wood in conjunction with slight bending of the teeth. As the load increased, the back of the plate began to lift away from the surface of the wood, causing the teeth in that area to become virtually ineffective in resisting load. Near the ultimate load, the wood fibers at the tooth-wood interface began to deform plastically due to the large loads transmitted by the metal plate connector through the teeth and into the wood. Gupta and Gebremedhin (1990) observed a similar failure mode in their study of MPC TSJs.

Because of the nonlinear shapes of the load-deflection curves, which made it difficult to define a single valued stiffness, the yield point for each joint was defined at the design strength (one-third of the ultimate strength for that particular joint) ("National" 1991). To calculate the stiffness (secant stiffness), one-third of the ultimate strength of the joint was divided by the corresponding deflection. For the earthquake simulations (Northridge and artificial earthquakes), this point occurred after the earthquake loading.

### Static Tests

The mean static strength of the control group for batch 1 was 32.4 kN with a coefficient of variation (COV) of 6%. The average yield displacement was 0.15 mm. The mean stiffness for the control group was  $0.76 \times 10^5$  N/mm with a COV of 16%. The mean static strength of the control group for batch 2 was 29.9 kN with a COV of 8%. The mean stiffness for batch 2 was  $0.49 \times 10^5$  N/mm with a COV of 14%. The average yield displacement was 0.20 mm.

There is strong statistical evidence that the TSJs constructed from the two different batches of plates have neither the same mean strength nor the same mean stiffness (two side p-values of 0.025 and 0.007 for strength and stiffness comparisons, respectively). Thus, the statistical evidence suggests that strength and stiffness comparisons should be made between joints fabricated from the same batch of metal plate connectors. To determine the strength and stiffness degradation, if any, caused by a particular earthquake or cyclic loading, the statistical test should include the control group that was fabricated from the same batch of plates.

Specific gravity and moisture content values for the control groups using plates from batch 1 and batch 2 cannot be statistically separated at the 0.05 level of significance. This evidence suggests that the differences in strength and stiffness between the two control groups are not due to differences in the wood. It is more likely that characteristics of the metal plate connectors themselves caused the differences in strength and stiffness between the static loading tests of the two different batches. Some of the physical and mechanical charac-

TABLE 3. Summary of Tension-Splice Joint Test Results

Test (1)	N (2)	Mean strength (kN) (3)	Mean stiffness ( $10^5$ N/mm) (4)	SG (5)	Average displacement failure (mm) (6)	Yield displacement (mm) (7)	MC (8)	Mean wood MOE (GPa) (9)	Failure mode (10)
Control group (batch-1)	9	32.4 (6)	0.76 (16)	0.50	2.92 (25)	0.15	13.0 (5)	ND	8-TW, 1-PF
Control group (batch-2)	9	29.9 (8)	0.49 (14)	0.48	2.45 (17)	0.20	13.4 (4)	12.4 (5)	TW
Northridge earthquake simulation	10	33.7 (7)	0.70 (14)	0.50	4.70 (12)	0.15	14.5 (12)	12.8 (12)	8-TW, 2-PF
Artificial earthquake simulation	9	28.8 (13)	0.61 (15)	0.48	2.34 (18)	0.15	13.4 (4)	12.3 (7)	TW
Sequential phased displacement	8	32.0 (5)	0.33 (14)	0.50	2.29 (30)	0.33	13.6 (3)	12.4 (8)	TW
Cyclic loading	20	Varies*	Varies*	0.45			12.6	12.1 (6)	TW

Note: ND: Not determined; TW: tooth withdrawal; PF: plate failure; SG: mean specific gravity; MC: moisture content. Numbers in parentheses are coefficients of variation in percent.

\*Depends on the cyclic amplitude (Fig. 11).

teristics that could cause strength differences between the two batches of plates are yield point, surface roughness, die age, and steel grade.

### Northridge Earthquake Tests

Analysis of the data suggests that the TSJs did not degrade in either strength or stiffness when subjected to the Northridge earthquake time history used in this simulation. The mean strength and stiffness of the joints (after being subjected to the earthquake loads), on application of the ramp load, were 33.7 kN with a COV of 7% and  $0.70 \times 10^5$  N/mm with a COV of 14%, respectively.

A statistical comparison of these results with the static loading control group (batch 1) suggested that the Northridge earthquake load time history did not degrade the strength or stiffness of the TSJs (two-sided p-values of 0.78 and 0.28 for strength and stiffness degradation, respectively).

The lack of strength and stiffness degradation from the Northridge earthquake tests is not surprising. As shown in Fig. 3, the maximum load developed in the TSJ during the earthquake simulation (5.5 kN) is only 17% of the average ultimate load for TSJs (32.4 kN, batch 1).

### Large Artificial Earthquake Tests

The average strength and stiffness of the TSJs after being subjected to the artificial earthquake load time history were 28.8 kN with a COV of 13% and  $0.61 \times 10^5$  N/mm with a COV of 15%, respectively. Strength and stiffness degradation did not occur as a result of the artificial earthquake when compared to the static strength for batch 2 plates (two-sided p-values of 0.49 for strength degradation and 0.18 for stiffness degradation, respectively).

The absence of strength and stiffness degradation from the earthquake simulation tests can be explained. As shown in Fig. 4, the maximum load developed in the TSJ during the artificial earthquake simulation (6.6 kN) is less than 22% of the average ultimate load for TSJs (29.9 kN for batch 2). Larger amplitude loads or repeated applications of the earthquake time history may, however, cause strength degradation in TSJs. But the artificial earthquake ground accelerations were, intentionally, very large (1.0 g maximum horizontal acceleration, 0.67 g maximum vertical acceleration). Therefore, much larger amplitude forces applied to a TSJ are unlikely. Although, at this point, the effect of repeated applications of a large artificial earthquake time history is unknown, it is possible that strength and/or stiffness degradation would occur.

### Sequential Phased Displacement Test

The average strength and stiffness of the TSJs subjected to the SPD loading and then caused to fail under a static ramp load were 32 kN with a COV of 5% and  $0.33 \times 10^5$  N/mm with a COV of 14%, respectively. A statistical analysis, compared with the static loading control group from batch 1, indicates that the SPD loading did not significantly reduce the mean strength of the TSJs (two-sided p-value of 0.63); however, stiffness degradation did occur as a result of the SPD loading (two-sided p-value = 0.000).

Control difficulties were encountered during the SPD tests. The difference between the maximum tensile load and the maximum compressive load in each cycle could approach as much as 62.3 kN. This difference required a loading rate of 125 kN/s, which appeared to be near the maximum capabilities of the testing system. The effect of operating near the limits of the hydraulic system was a significant decrease in control. Also, the deflection feedback loop was controlled by LVDTs that had an approximate resolution of 0.02 mm. A higher res-

olution would have been preferred to tighten the control of the deflection feedback loop when working with such stiff connections.

Generally, the compressive loads tend to increase at a higher rate than the tensile loads with time, as the TSJ is stiffer in compression than tension. Also, the deflection tends to be symmetrical during the test, following the prescribed sequential phased displacement loading.

Because the compressive loads on the TSJs during the SPD loading were so large (up to 46.7 kN), there was some out-of-plane movement of the joint. As the compressive load increased, the TSJ tended to move downward slightly (less than 6.6 mm). Therefore, a moment was created at the connection. Because there was no statistical evidence of strength degradation as a result of the SPD loading, it can be assumed that the out-of-plane movement had no significant effect on the strength of the TSJs.

The following dynamic properties, as defined by Dolan (1994), for TSJs were evaluated using the SPD method: energy dissipation, equivalent viscous damping ratio, and cyclic stiffness. These dynamic properties are described as follows and computed from individual hysteresis curves. Recall that the amplitudes of the cycles in the SPD loading are defined in terms of displacement as a percent of the yield displacement. The dynamic properties of MPC TSJs are then plotted against the deflection as a percent of the yield displacement. The percent of yield displacement is defined as the maximum displacement in the hysteresis curve being analyzed divided by the yield displacement from the static loading control group (0.15 mm, batch 1).

The hysteresis curve used in this study for calculation of the dynamic properties was not necessarily the stabilized hysteresis curve. The SPD method defines a stabilized cycle as one in the set of stabilizing cycles (defined in Fig. 6) that has a load degradation of no more than 5% from the preceding cycle. Because of the control difficulties discussed previously, it was not possible to apply this definition of a stabilized hysteresis curve to these tests on TSJs. The testing system was able to control the deflections only within 4–7% of the target deflection. Therefore, the third cycle in each set of stabilization cycles was arbitrarily used as the stabilized hysteresis curve to plot the hysteresis curve used for calculation of the dynamic properties. For nailed and bolted connections in wood, Dolan (1994) found that only three cycles were necessary to obtain a stabilized hysteresis curve. Henceforth, in this paper, the third cycle in the set of three stabilizing cycles is referred to as the stabilized cycle and is used to compute the dynamic properties.

Energy dissipation is the area enclosed by the load-deflection trace. Because TSJs may behave differently in tension and compression, energy dissipation in tension ( $EA_t$ ) and energy dissipation in compression ( $EA_c$ ) were calculated separately. Energy input in tension ( $EI_t$ ) and energy input in compression ( $EI_c$ ) were also determined as in Dolan (1994). With the preceding definitions of energy dissipation and energy input, the damping ratios for tension and compression,  $\xi_t$  and  $\xi_c$ , respectively, for any given cycle, may be approximated by the following formulas (Dolan 1994):

$$\xi_t = EA_t / 2\pi \cdot EI_t \quad (1)$$

$$\xi_c = EA_c / 2\pi \cdot EI_c \quad (2)$$

A digitizing tablet (Calcomp Digitizer Products Division, Scottsdale, Ariz., Model No. 33120) was used to calculate the areas enclosed by the tensile and compressive regions of the hysteresis curves. Typical plots of the energy dissipation and damping ratio as functions of the displacement (percent of yield displacement) are shown in Fig. 8 and 9, respectively,

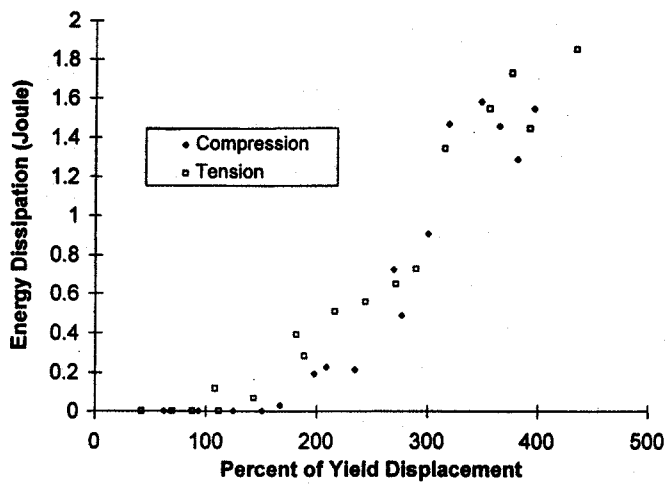


FIG. 8. Energy Dissipation in Typical Tension-Splice Joint during SPD Loading

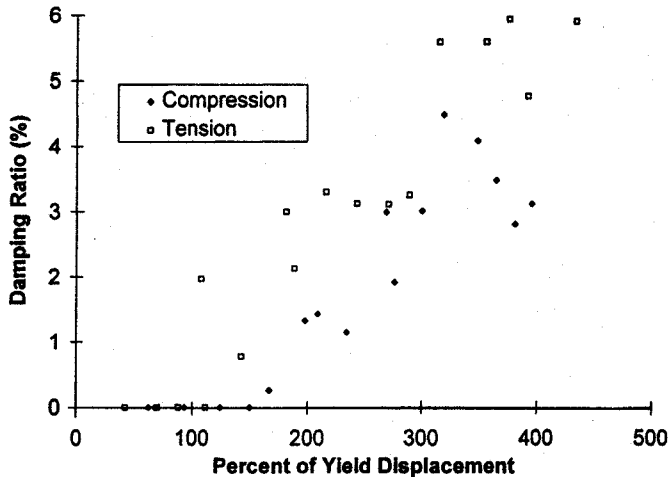


FIG. 9. Damping Ratio in Typical Tension-Splice Joint during SPD Loading

for one typical joint. Each point on the graph is calculated from a hysteresis curve developed during the SPD loading.

Currently, there is no standard to determine a design level damping ratio from the SPD loading. For this study, it was decided to compute the damping ratio associated with the first stabilized hysteresis curve to have a maximum tensile load equal to, or exceeding, the design load for the TSJ (approximately 33% of the average ultimate load, 10.7 kN). Because TSJs are not actually designed for compressive loads, only the damping ratio associated with tensile loads is presented. Based on the above definition of design levels, a damping ratio of 4.3% was determined for the TSJ. This value is very close to the 5% damping ratio typically assumed for the design of wood structures. Because of the control difficulties, only three tests produced hysteresis curves from which the energy dissipation and damping ratio could be measured. In some cases, a more detailed examination of Fig. 9 is suggested. Factors to consider are the number and amplitude of the cycles the TSJ is expected to experience in service. It may be appropriate to select the damping ratio (from Fig. 9) associated with the specific level of displacement expected for the joint in service.

Cyclic stiffness is defined (Dolan 1994) as the slope of a straight line drawn between the lower left of the hysteresis curve to the upper right of the hysteresis curve, passing through the lowest and highest points. However, MPC TSJs have different stiffnesses in the compressive and tensile directions; therefore, in this paper, cyclic stiffnesses for tension and compression are defined separately. A plot of the cyclic stiff-

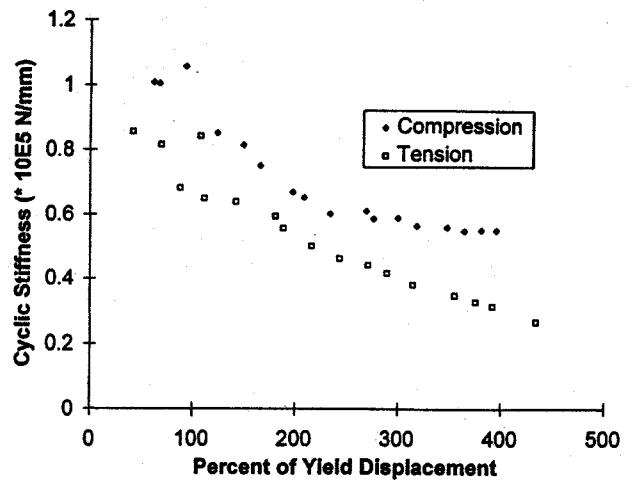


FIG. 10. Cyclic Stiffness in Typical Tension-Splice Joint during SPD Loading

ness as a function of the displacement as a percent of yield displacement (0.15 mm, defined from the static tests for batch 1) is shown in Fig. 10 for a typical joint. From this plot, it is clear that stiffness degradation does occur as the SPD loading progresses to greater displacement amplitudes because of the accumulated damage in the wood fibers at the tooth-wood interface.

In Figs. 8 and 9 the energy dissipation and damping ratio generally tend to increase with increasing displacement (percent of yield displacement) during the SPD loading. Cyclic stiffness (Fig. 10) generally tends to decrease with increasing displacement (as a percent of yield displacement) during the SPD loading.

#### Cyclic Loading Tests

The overall results for the cyclic loading tests are plotted in Fig. 11. The vertical axis (strength ratio) is the ratio of the strength of the TSJ under a static ramp load after completion of the 200 cycles to the average strength of the static loading control group for batch 2. The horizontal axis (cyclic amplitude) is the amplitude of the cycles divided by the average strength of the static loading control group for batch 2 (29.9 kN) and expressed as a percentage (see Fig. 7 for the actual cyclic loading function). For a joint to be assigned a nonzero postcyclic loading strength, it must be able to carry load after the conclusion of the 200 cycles. Joints that failed during the cyclic loading were assigned a zero strength ratio. The results for the static loading control group (batch 2) are plotted on Fig. 11 at 0% cyclic amplitude. There appears to be a distinct threshold between 20 and 25% cyclic amplitude where TSJs are no longer able to survive the entire set of cycles.

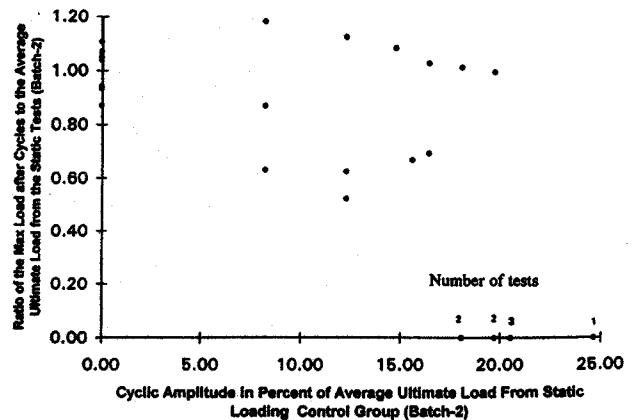


FIG. 11. Cyclic Loading Test Results for Tension-Splice Joints

TABLE 4. Summary of Heel Joint Test Results

Test (1)	N (2)	Mean strength <sup>a</sup> (kN) (3)	Mean axial stiffness (10 <sup>5</sup> N/mm) (4)	Mean rotational stiffness (10 <sup>6</sup> N-m/radian) (5)	Average deflection at maximum load (mm) (6)	Average top chord yield displacement (mm) (7)	Mean specific gravity (8)	Mean moisture content (%) (9)	Mean wood MOE (GPa) (10)
Control group (static tests)	9	27.6 (7)	0.63 (61)	5.89 (54)	5.66 (21)	0.18 (39)	0.51	14.3 (11)	13.9 (8)
Artificial earthquake simulation	10	26.9 (8)	0.25 (54)	3.65 (68)	7.70 (10)	0.43 (34)	0.53	13.0 (4)	13.8 (8)
Sequential phased displacement	8	18.6 (16)	0.24 (57)	9.49 (70)	3.81 (38)	0.36 (53)	0.48	12.9 (6)	13.4 (8)
Cyclic loading	27	Varies <sup>b</sup>	Varies <sup>b</sup>	Varies <sup>b</sup>	—	—	0.51	12.7 (12)	14.4

Note: N: sample size. Numbers in parentheses are coefficients of variation in percent.

<sup>a</sup>Maximum force in top chord.

<sup>b</sup>Depends on the cyclic amplitude (Fig. 15).

## Heel Joints

Strength, stiffness, specific gravity, and moisture content results for all HJ tests are shown in Table 4, along with deflections at maximum load, yield displacements, and moduli of elasticity. Mean strength for the cyclic loading tests is not given in this table because of the strength dependence on the amplitude of the cycles.

The dominant failure mode for the HJs was tooth withdrawal. This mode occurred as a result of the wood being crushed by the side of the tooth near the surface of the wood in conjunction with slight bending of the teeth as the plate deformed in shear. As the load increased, the corners of the plate began to lift away from the surface of the wood, causing the teeth in that area to become virtually ineffective in resisting load. In instances where the member failed near the grips (not near the metal plate connector), the results were discarded (one sample during the static loading control group and two samples during the sequential phased displacement loading). Large shear deformation of the plate was apparent. Gupta and Gebremedhin (1990) observed similar failures in their study of MPC HJs.

To calculate the axial stiffness for each joint (secant stiffness), one-third of the ultimate load in the top chord of the HJ was divided by the corresponding deflection of the top chord with respect to the bottom chord. To calculate the rotational stiffness (secant stiffness), one-third of the ultimate moment for each joint was divided by the corresponding rotation. For the artificial earthquake simulation, this point occurred after the earthquake loading. A rotational slip criteria was not considered in determining the design moment of the HJs. Yield point was defined at the deflection corresponding to one-third of the ultimate strength of the joint.

### Static Tests

The mean strength for the static loading control group was 27.6 kN with a COV of 7%. The mean axial stiffness of the top chord for the control group was  $0.63 \times 10^5$  N/mm with a COV of 61%. The mean rotational stiffness for the control group was  $5.89 \times 10^5$  N-m/rad with a COV of 54%. The mean yield points for axial deflection and rotation were at 0.18 mm and 0.0009 rad, respectively.

The shapes of the load-deflection and moment-rotation curves were rather inconsistent. Often, the LVDT measuring the deflection of the top chord did not register any movement until the load exceeded 4 kN. This may be attributed to the joint experiencing an initial rotation of the top chord with respect to the bottom chord, rather than pure axial movement of the top chord. This caused the stiffness variation to be extremely high. Also, the shapes of the moment-rotation curves were very inconsistent. In some cases, the angle between the top and bottom chord decreased until a specific load and then began to increase, which was most likely due to a very slight

eccentric alignment of the load, applied by the hydraulic cylinder, to the top chord (load not applied directly through the centerline of the top chord of the heel joint). The axial stiffness of the top chord ranged from a low of  $0.32 \times 10^5$  N/mm to a high of  $1.57 \times 10^5$  N/mm. The large COVs associated with the axial and rotational stiffnesses reflect the inconsistencies in the load-deflection and the moment-rotation curves.

### Large Artificial Earthquake Tests

The average strength (top chord ultimate load) of the HJs after being subjected to the artificial earthquake force time history was 26.9 N with a COV of 8%. The average postearthquake loading axial and rotational stiffnesses were  $0.25 \times 10^5$  N/mm with a COV of 54% and  $3.65 \times 10^5$  N-m/rad with a COV of 68%, respectively.

No significant strength or rotational stiffness degradation occurred as a result of the artificial earthquake time history (two-sided p-values of 0.46 and 0.15 for strength and rotational stiffness, respectively). However, axial stiffness was reduced as a result of the artificial earthquake time history (two-sided p-value of 0.003).

### Sequential Phased Displacement Loading

The average strength (ultimate top chord load) of the HJs subjected to the SPD loading and then caused to fail under a static ramp load was 18.6 N with a COV of 16%. The average top chord axial and rotational stiffnesses were  $0.24 \times 10^5$  N/mm with a COV of 57% and  $9.49 \times 10^5$  N-m/rad with a COV of 70%, respectively. A statistical analysis indicated that the SPD loading significantly reduced the mean strength and axial stiffness of the HJs (two-sided p-values of 0.000 and 0.004 for strength and axial stiffness, respectively). However, significant rotational stiffness degradation did not occur as a result of the SPD loading (two-sided p-value of 0.190).

For HJs it was decided to compute the damping ratio associated with the first stabilized hysteresis curve to have a maximum compressive load in the top chord approximately equal to the design load (National 1991) for the top chord of the HJ (33% of the average ultimate load, 9.1 kN). Because HJs are not generally designed for tensile loads in the top chord (except for cantilevers), only the design level damping ratio associated with compressive loads in the top chord is presented. Because of control difficulties, only six tests produced hysteresis curves from which the energy dissipation and damping ratio could be measured. Based on the preceding definition of design levels, a damping ratio of 3.8% was determined for the HJs.

Dynamic properties for HJs were determined in the same manner as for the TSJ and are shown in Figs. 12–14 for a typical joint. The energy dissipation and damping ratio both tend to increase during the SPD loading. Cyclic stiffness clearly decreases with increasing displacement as a percent of

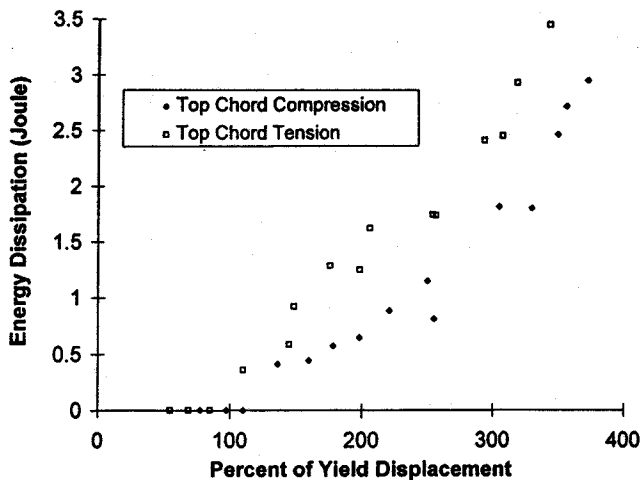


FIG. 12. Energy Dissipation in Typical Heel Joint during SPD Loading

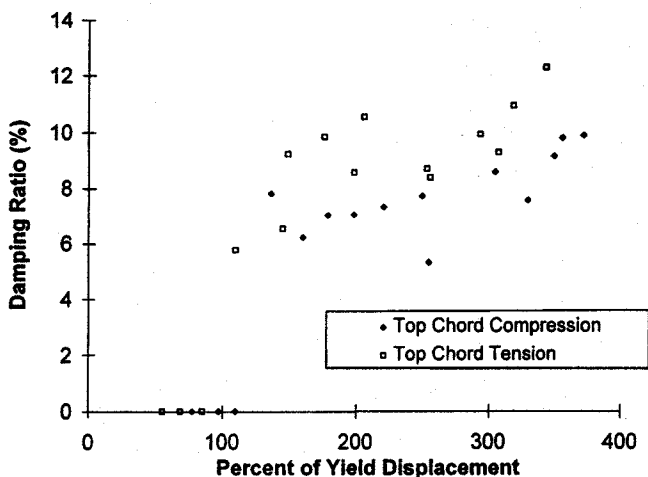


FIG. 13. Damping Ratio in Typical Heel Joint during SPD Loading

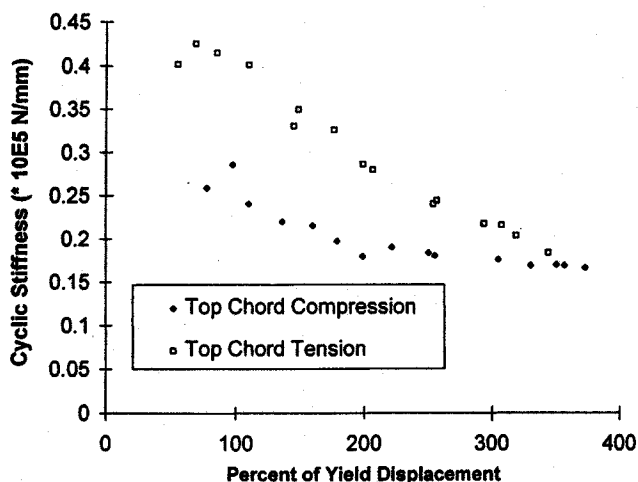


FIG. 14. Cyclic Stiffness in Typical Heel Joint during SPD Loading

yield displacement. This implies that the connection is accumulating damage at the tooth-wood interface.

#### Cyclic Loading Test

The overall results for the cyclic loading tests are plotted in Fig. 15. A threshold appears to exist at approximately 35% cyclic amplitude where heel joints are no longer able to sur-

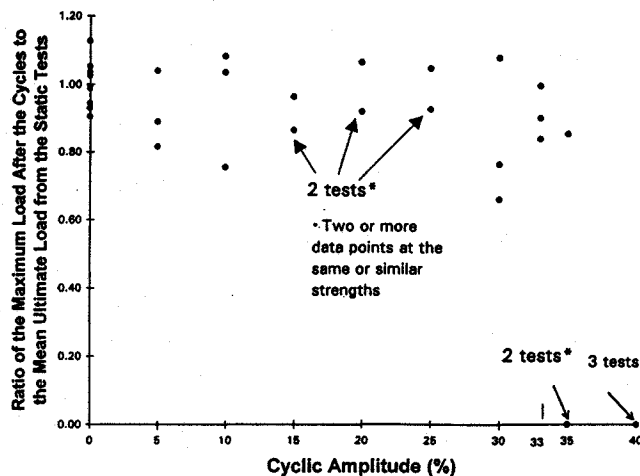


FIG. 15. Cyclic Loading Test Results for Heel Joints

vive the entire set of cycles. From the cyclic tests, it is evident that caution should be applied when using MPC joints in situations where cyclic loading is prevalent, such as in high wind areas, bridges, and floors. Although the cyclic loading investigated in this study loaded the MPC joints beyond their design range, it is possible that lower level cyclic loads may also have an effect on the strength after a large number of cycles.

#### CONCLUSIONS

The Northridge and large artificial earthquakes forces caused no strength or stiffness degradation when compared to the control groups of static tests fabricated from similar plates. Dynamic properties of MPC TSJs and HJs are shown to be dependent on the level of displacement in the SPD loading. As the displacement increases, damage accumulates in the connection causing the damping ratio and energy dissipation to increase and the cyclic stiffness to decrease. For design, damping ratios of 4.3% for the TSJ and 3.8% for HJs, respectively, are suggested, based on the sequential phased displacement tests. The cyclic loading used in this study has a significant effect on the strength of TSJs. There appears to be a threshold between 20 and 25% cyclic amplitude for the TSJs and at approximately 35% cyclic amplitude for the HJs beyond which the joints cannot survive 200 cycles.

#### ACKNOWLEDGMENT

Funding for this research was provided by the United States Department of Agriculture, National Research Initiative, Competitive Grants Program.

#### APPENDIX I. REFERENCES

- Buchanan, A. H., and Dean, J. A. (1994). "Practical design of timber structures to resist earthquakes." *Proc., Pacific Timber Engrg. Conf., Timber Res. and Devel. Advisory Council, Queensland, Australia*, 813-822.
- Dagher, H. J., Caccese, V., Hsu, Y., Wolfe, R., and Ritter, M. (1991). "Feasibility of metal connector plates in timber bridges: fatigue study." *Tech. Rep.*, Dept. of Civ. Engrg., Univ. of Maine, Orono, Maine.
- Dolan, J. D. (1994). "Proposed test method for dynamic properties of connections assembled with mechanical fasteners." *J. Testing and Evaluation*, 22(6), 542-547.
- Emerson, R. N., and Fridley, K. J. (1996). "Resistance of metal-plate-connected truss joints to dynamic loading." *Forest Products J.*, 46(5), 83-90.
- Foliente, G. C., and Zacher, E. G. (1994). "Performance tests of timber structural systems under seismic loads." *Proc., Res. Needs Workshop on Anal., Des., and Testing of Timber Struct. under Seismic Loads*, G. C. Foliente, ed., Forest Products Lab., Univ. of California, Berkeley, Calif., 21-86.
- Gupta, R., and Gebremedhin, K. G. (1990). "Destructive testing of metal-

plate-connected wood truss joints." *J. of Struct. Engrg.*, ASCE, 116(7), 1971-1982.

Gupta, R., Vatovec, M., and Miller, T. H. (1996). "Metal-plate-connected wood truss joints: a literature review." *Res. Contribution 13*, Forest Res. Lab., Oregon State Univ., Corvallis, Oreg.

Hayashi, T., Sasaki, H., and Masuda, M. (1980). "Fatigue properties for wood butt joints with metal plate connectors." *Forest Products J.*, 30(2), 49-54.

Kent, S. M. (1996). "Dynamic behavior of metal-plate-connected wood truss joints," MS thesis, Oregon State Univ., Corvallis, Oreg.

*National design specification for wood construction.* (1991). Nat. Forest and Paper Assn., Washington, D.C.

"National design standard for metal-plate-connected wood truss construction." (1995). *ANSI/TPI 1-1995*, ANSI, Madison, Wisc.

*SAP90: a series of computer programs for finite element analysis of structures.* (1995). Computers and Structures, Inc., Berkeley, Calif.

Silva, W. J., and Lee, K. (1987). "State-of-the-art for assessing earthquake hazards in the US: WES-RASCAL code for synthesizing earthquake ground motions." *Miscellaneous Paper S-73-1*, U.S. Army Corps of Engineers, Washington, D.C.

Sletteland, N. T., Pratt, G. L., and Schuler, R. T. (1977). "Fatigue life of metal plate connector plates." *ASAE Paper No. 77-4037*, Am. Soc. of Agric. Engrs., St. Joseph, Mich.

*Standard test methods for direct moisture content measurement of wood*

*and wood-base materials; D4442-92.* (1996a). ASTM, West Conshohocken, Pa., 485-489.

*Standard test methods for mechanical fasteners in wood; D1761-88.* (1996b). ASTM, West Conshohocken, Pa., 348-355.

*Standard test methods for specific gravity of wood and wood-base materials; D2395-93.* (1996). ASTM, West Conshohocken, Pa., 348-355.

"Structural engineering design provisions." (1994). *Uniform Building Code, Vol. 2.* International Conference of Building Officials, Whittier, Calif.

Tokuda, M., Takeshita, M., and Sugiyama, H. (1979). "The behaviors of metal plate connector joints subjected to repetitive tension force." *J. Japan Wood Res. Soc.*, Tokyo, Japan, 25(6), 408-413.

## APPENDIX II. NOTATION

*The following symbols are used in this paper:*

$EA_c$  = energy dissipation in compression;  
 $EA_t$  = energy dissipation in tension;  
 $EI_c$  = energy input in compression;  
 $EI_t$  = energy input in tension;  
 $\xi_c$  = damping ratio for compression; and  
 $\xi_t$  = damping ratio for tension.